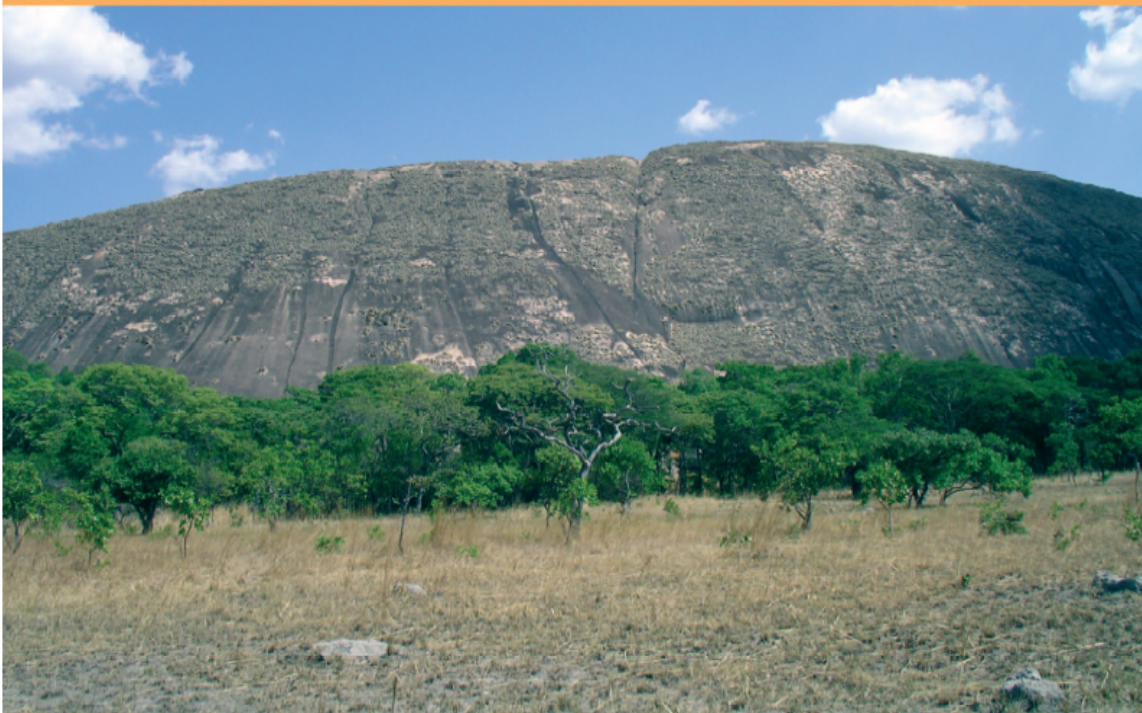


TANZANIA

Journal OF Earth Sciences

Geological Survey of Tanzania



■ Volume 1 ■ December 2009

CONTENTS

Appraisal of the Stratigraphy and mineral potential of Tanzania.

Mruma A. H., Semkiwa P., Temu E. B., Minde, A......2-28

Neoproterozoic inheritance during Cainozoic rifting in the western and south western branches of the East African rift system: evidence from carbonatite and alkaline intrusions.

Mbede E., Kampunzu A. B. & Armstrong R. A......29-37

Active faults and fault segmentation in Dodoma area, Tanzania. A first assessment of the seismic invents in the area.

Athanas S. Macheyeke A., Delvaux D., De Batist M. & Mruma A......38-57

Origin of the arc structure of the supracrustal rocks of the Sukumaland Greenstone Belt, Tanzania.

Mruma A.H. and Ngassala S......58-65

Integration of geo-exploration datasets (Geological, Geochemical and Geophysical) for Mineral Exploration in a GIS: Case Study in Golden Ridge Project, Tanzania.

Makene C.K+.....66-74

Multi-structures of a single deformation phase in the Sukumaland Greenstone Belt.

Mruma A.H......75-86

Impacts of artisanal small-scale gold mining – Mercury contamination of food crops cultivated in Mgusu, Geita District in Tanzania.

Kinabo C. and Lyimo E......87-95

Three-dimensional gravity modelling of the magmatic segments within the main Ethiopian Rift.

Mickus K, Ketsela T., Keller G. R. & Befekadu O......96-106

Stress regimes in eastern and southern Africa.

Lostina S. Chapola107-120

The Malagarasi Riverine Limnology

Nkotagu, Hudson H. and Athuman, Charles B......121-132

© Copy right 2009 by the Geological Survey of Tanzania. All rights reserved. No part of this publication may be reproduced, stored in a retrieval system, or transmitted, in any form or means, including electronics, photographic, mechanical.

**Active faults and fault segmentation in the Dodoma area, Tanzania:
A first assessment of the seismic hazard in the area**

Athanas S. Macheyeke(1,3,5), Damien Delvaux(2), Marc De Batist (1), Abdulkarim H. Mruma(4,5)

(1) Renard Center for Marine Geology, Universiteit Gent B-9000 Gent, Belgium E-mail:
asmacheyeke@yahoo.com

(2) Royal Museum for Central Africa, B-3080 Tervuren, Belgium (3) Mineral Resources Institute, P. O. Box 1696 Dodoma, Tanzania (4) Geological Survey of Tanzania, P.O.BOX 903, DODOMA (5) The University of Dar es Salaam, Department of Geology, P.O. Box 350052 DSM

ABSTRACT

Dodoma, the capital of Tanzania, was hit by a 5.5 magnitude (M_w) earthquake during a parliamentary session on November 4, 2002. It was part of a seismic crisis with 37 events of magnitude (M_w) ranging from 3.7 to 5.5., from early 2001 to late 2004 and centered about 80 km north of Dodoma. This paper re-evaluates the active tectonic setting of the Dodoma area, using combined integration of existing geological and topographic maps with the recently released SRTM DEM with a GIS. Main emphasis is put on morphotectonic analysis of potentially active fault scarps using topographic elevation data extracted from the SRTM DEM. The ongoing study has revealed that the Mponde and Bubu faults are seemingly the active faults or most likely so as compared to other faults in the Dodoma area.

The Saranda and the Bubu faults have three fault segments each. For the Saranda fault, the fault segments are hereby called Saranda south (>11 km), Saranda mid (29 km) and Saranda north (24 km). The Gongga (42 km), Makutupora (30 km) and Nkambala (33 km) are fault segments which form the Bubu fault. Similarly, the Hombolo fault has two fault segments namely the Dam fault segment (18 km) and the Nzuguni fault segment (> 19 km) with total length of the order of 40 km. similar investigations on the Fufu fault are underway. It follows therefore that, according to Wells and Coppersmith (1994), the faults in the Dodoma area, assuming fully reactivation, can independently produce earthquakes of magnitudes ranging from about $M_w = 6.95$ to $M_w = 7.20$ Key words: Tanzania, Dodoma, fault segmentation, displacement profile, seismic hazard.

INTRODUCTION

On November 4, 2002, Dodoma, the capital of Tanzania, was hit by a $M_w = 5.5$ earthquake during a parliamentary session. It was the peak of a seismic crisis with an earthquake swarm centered in the Chenene Mountains, about 80 km north of Dodoma town, with 37 events of magnitude M_w ranging from 3.7 to 5.5., from early 2001 to late 2004. The majority of them lie along the Chenene Mountain, within an area between the Bubu fault and the antithetically dipping Hombolo fault.

This swarm occurred in a poorly defined portion of the East African rift system, linking in a diffuse way the southern termination of the Kenya rift in northern Tanzania, to the Tanganyika-Nyasa rift in the Rungwe volcanic region at Mbeya (Iranga, 1991). It also raised questions regarding the assessment of active tectonic manifestations in the Dodoma region, which is located along the eastern margin of the Tanzanian Archaean craton, close to the Mozambique belt (Fig. 1).

The main objective of this study is to identify possible active faults using 90 m resolution shuttle radar topography mission (SRTM) data and to evaluate the seismic risk in the Dodoma area and the surroundings. This involved a morphotectonic re-evaluation of the surface expression of the faults and estimating their associated vertical offsets. The latter is done using the supposedly displaced topographic surface taken as a reference along regularly spaced topographic profiles extracted from the SRTM DEM at a high angle to the related fault. The values obtained are plotted with distance along the trend of the fault to produce relative displacement profiles. These are interpreted in terms of fault growth and segmentation. The possible maximum earthquakes which can be generated by such fault segments in the area using the empirical relations of Wells and Coppersmith (1994) have been presented.

The determination of the maximum possible magnitude for future earthquakes is of major importance for the estimation of the seismic risk of any seismically active area. Analysis of past events recorded historically or instrumentally gives some indications, but which are generally incomplete as the observation period might be short regarding to the seismic cycle. Therefore detailed paleoseismic investigations are necessary to ensure a proper time span coverage of past seismic activity.

With this regards, the determination of fault segmentation has a particular importance in seismic risk analysis as it might reduce the maximum possible magnitude on a particular fault system.

Fault segments in their early stages of formation occur as individual fault strands with displacement profiles that decrease from maximum in or near the center to zero at either tips (Young et al 2001, Burbank and Anderson 2001). Faults can grow by radial propagation (Cartwright et al (1995), Burbank and Anderson 2001), i.e. the individual fault segments strand simply lengthens and accumulates more displacement, while maintaining the standard displacement profiles (Fig. 2). Faults can also grow by segment linkage (Burbank and Anderson 2001), when different individual fault segments become connected as they grow laterally, overlap and become hooked to each other on tips (Young et al., 2001; Burbank and Anderson 2001; Fig. 2) in a process which is referred to as fault interaction. According to Burbank and Anderson (2001), the maximum displacement of a resulting fault is 9 % larger than that of a similar isolated fault, for overlapping fault segments of length 'a' when spaced $0.05a$ from each other. Such interactions may promote or inhibit fault nucleation and growth, distort fault slip profiles, produce fault linkage and coalescence, and collectively result in populations of faults with distinctive characteristics (Peacock and Sanderson 1991).



Fig. 1. Location of the study area in the framework of the East African Rift system and its associated structures in Tanzania (after Iranga, 1991).

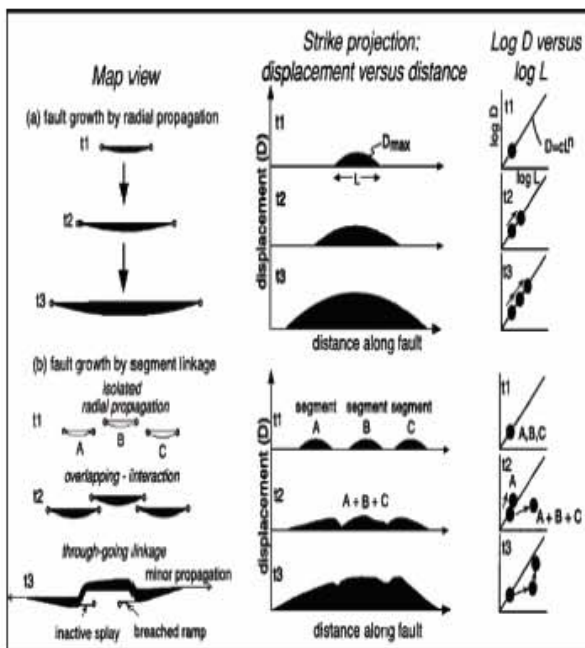


Fig. 2. Two models of fault growth. During fault growth by radial propagation (a), an individual fault simply lengthens and accumulates more displacement through time 't'. Plots of displacement versus fault length (right column) show a steady increase in displacement as the fault grows. Map view on the left (b) shows a different scheme of fault growth, in which small individual faults

gradually link up to create one large, through-going fault. Whereas the accumulation of displacement follows a predictable path for individual segment when they link up, displacement becomes considerably less than that predicted for a fault of this length (see right-hand column). Through time, the slip deficiencies near the point of segment linkage are reduced. Ultimately, the only indication that the large fault resulted from fault linkage of smaller ones may be the presence of perturbations to the smooth, bow-shaped displacement near the former zones of overlap and linkage (from Burbank, and Anderson 2001).

The phenomenon of fault-zone segmentation has been recognized for over 20 years (Keller and Pinter 2002). Seismotectonics studies show that it is commonly one or two fault segments that are involved in rupturing during large seismic events, each fault segment rupturing independently of the other, each with its own rupture history (Zhang et al 1998). Ruptures that occur along the entire length of a long fault are much rarer (Keller and Pinter 2002). Therefore, for evaluation of both past and future earthquakes, the study of fault segments using geologic data from paleoseismological sites (from both stratigraphic and geomorphic evidence) is essential (Piccardi 2005).

Segment boundaries are commonly characterized by complex fault-zone geometry consisting of step-overs, jogs, bifurcations, bends, gaps, and other patterns that create both 'geometric discontinuities' and 'structural discontinuities' within a fault zone (Zhang et al 1998). The structural discontinuities of a fault zone may potentially act as structural barriers that influence earthquake rupture initiation and termination, and may impede or stop earthquake rupture propagation (Zhang et al 1998). Small-scale structural discontinuities (< 1 km) are, however, probably not capable of stopping an earthquake rupture with more than 30 km length or magnitude 7 or larger (Crone and Halle 1991).

Therefore, the size of a structural discontinuity with respect to the rupture length or displacement may play an important role in controlling rupture termination.

As concluded by Iranga (1991) in his work: ‘...if there is a certain tectonic zone characterized by some peculiarity in its tectonic history and structure, and if earthquakes of certain type have occurred in the past somewhere in this zone, then it may be assumed that earthquakes of similar characteristics may arise along the length of this zone’.

GEOLOGICAL SETTING

The Dodoma area located in central Tanzania is part of the Tanzanian Archaean craton consisting of granulated and sheared synorogenic granites; and also unsheared late-orogenic granites (Fig. 3). The Dodoman granite belt occupy the central part of the granitoid Tanzanian Shield, which was formed by migmatitisation and then further stabilized by a succession of granitic intrusion (Wades and Oates 1938; Fozzard 1962; Barth 1996).

Whole rock radiometric dating of the Tanzanian craton, indicates the ages of the migmatites and granitic complexes of the Dodoman range between the time of the last metamorphism of the Dodoman gneisses (2.5Ga) and intrusion event of the post-Nyanzian intrusive granites (1.87Ga), whereas age greater than 2.8Ga are absent, thus demonstrating unique Archaean event at 2.5Ga (Wendt et al 1972; Gabert 1973; Gabert and Wendt 1974; Bell and Dodson 1981). The Tanzanian craton is bounded to its eastern side by the Mozambique belt. Recent zircon age and Sm-Nd whole rock data indicate that it mainly consists of Archaean and Palaeoproterozoic gneisses that were reworked during the Pan-African (Pan-African) Orogeny (Vogt et al., 2006).

The dominant structural trend of the Dodoman tectonic domain is N120°-300°E, with some fluctuations, best

expressed in quartzitic rocks. Generally the region of investigation has a complex network of tectonic structures, most of which are Precambrian in origin. Recent structures associated with the rift system are locally well expressed, often reactivating Precambrian structures (Fairhead and Stuart 1982).

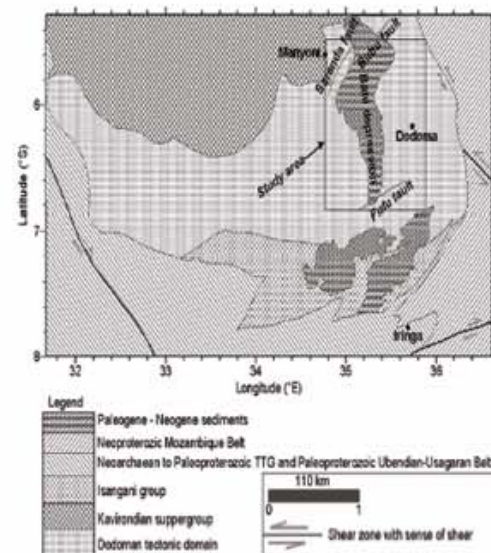


Fig. 3. Simplified regional geology map of the study area in relation to the surrounding geological units (Modified after Pinna et al 2004).

Covering the Dodoman rocks, the Kilimatinde Cement is the oldest sedimentary formation. It is a dominantly silcrete formation composed of silicified sandstone, but locally it can also be a calcrete or a ferricrete. Fozzard (1961) considers it to be formed in shallow evaporative basins developed on a quasi-planar land surface, between residual hills. Where eroded down to the weathered basement, the Kilimatinde Cement has a thickness of 15 to 30 m. In the Bahi depression, the Kilimatinde Cement is overlain by about 75 m thick Lake Beds of possible Plio-Pleistocene age. Therefore the age of the Kilimatinde Cement might go down to the Miocene-Early Pliocene. In most places, the Kilimatinde Cement is overlain by white sand soils (podzols), which is typical of sedimentary environments of low relief and high water table (Thomas

1994).

The area under investigation is located within the eastern branch of the East African rift system (Fig. 21), the most extensive currently active zone of the continental rifting on the globe (Shudofsky 1985, Brown and Girdler 1980). Current seismic activity suggests that the rift system is still active and indeed continues southerly (Shudofsky 1985). Much of the East African crust and uppermost mantle retains its pre-rift state, characterized by the absence of a well developed asthenosphere and a geotherm appropriate to a continental shield. This accounts for the widespread occurrences of the earthquakes at focal depths of 25-30 km which would otherwise be considered unusually deep if continental extension were occurring by lithospheric thinning and upward migration of the asthenosphere (Shudofsky 1985).

Late Tertiary rift faulting in the Dodoma area is not spectacular as in typical rift valley settings, but relief differences can be as high as 200 m between displaced blocks. With exception to the Sanzawa fault line, most morphologically expressed faults are displacing the Kilimatinde Cement, active during the Neogene rifting stage. When seen where basement is outcropping, they seem to reactivate pre-existing structural lines. This led to a lozenge pattern of normal faults bounding wide depressed areas.

The main NE-SW trending normal faults are from the northwest to the southeast; the Saranda, Bubu, Hombolo and Fufu faults show this. With exception of the Hombolo fault which dips westerly, other faults dip easterly. North of the area, the Mponde fault is N-S trending and joins southwards the NE-SE trending Saranda fault. A large morphological scarp runs NW-SE at the foot of the Chenene Mountains, probably following a pre-Kilimatinde Cement fault line but without morphological evidence for recent reactivation

(the Saranda fault). Instead, a discrete but sharp NW-SE trending topographic scarp runs at the margin of the Bahi depression, at the foot of the Chenene Mountains. It is located a few km SW of the Saranda fault and is attributed to a possible new active fault that we evidenced from the SRTM DELM, named here Maziwa fault from the name of a small village. Except for the Maziwa fault, these faults are characterized by scarp heights approaching 200 m.

The Dodoma area is characterized by moderate to large earthquake swarms whose focal mechanisms show a zone of distributed block faults and sub E-W extension (Brazier et al 2005). The earthquakes, essentially of mid-crustal depth, are broadly aligned in a NW-SE direction, more or less confined to the Chenene Mountains. However, the history of earthquakes in this area is neither continuous nor homogeneous (Iranga 1991), though evidences do exist that earthquakes in this area seem to occur throughout the rift floor and not entirely along narrow zone(s) (Baker 1965). So far, the Chenene Mountains appear to be most likely structurally controlled, but it is unclear whether the high topography of these mountain ranges has any contribution to the characteristic trend of these earthquake swarms or that the NW-SE structures such as the Sanzawa fault and the Maziwa structure (fault) control the pattern of the swarms. A few of these swarms have been reported to be destructive, for instance the November 4, 2002. This earthquake of Mw=5.5 whose epicenter was within the earthquake swarms area, left a few people dead, a school and a dispensary destroyed and the Tanzania parliamentary building cracked.

METHODOLOGY

The geology of the area of investigation is almost exclusively known from the existing 1:125,000 geological maps: QDS 123 Kwa Mtoro (Fozzard 1961), QDS 124 Kelema (Fozzard 1960), QDS 143 Meia Meia (or Maya Maya) (Julian et al 1963), QDS 142 Bahi

(Lounsberry et al 1967), as no extensive detailed work on the area has been reported later. The topographic coverage at 1:50,000 dates back to 1962-1963 or earlier, with contour lines every 50 feet (15 m). Air photographs cover is scarce and has not been used.

This work results mainly from the exploitation of the 90 m resolution SRTM data, the most recent digital elevation model (DEM) available released in 2004 for the African continent. The SRTM data are represented in map form with colour scale in function of the elevation and with artificial shading. These documents were geo-referenced and integrated in a Geographic Information System (GIS). With support of the GIS environment, the significant morphostructural signal was extracted from the SRTM-DEM in constant interaction with the geological and topographic maps, and the interpretation drawn on a new layer.

The SRTM-based DEM was also used for extracting digital topographic data along selected profiles drawn generally at a high angle from interpreted fault scarps. These topographic profiles were further studied in order to define the approximate topographic offset associated with the related faults.

By early 2006, a field campaign in the study area allowed to check and characterise the morphostructural interpretation obtained as described above.

Field investigation comprised also the inventory of hot springs found along active fault scarps, outcrop measurement of fault kinematic data for paleostress analysis, and trenching for paleoseismic investigation. The results of both the paleostress analysis and paleoseismic investigation will be reported elsewhere.

SRTM data: acquisition, processing, uses and limitation

The acquisition of SRTM is the result from a

collaborative effort by the National Aeronautics and Space Agency (NASA) and National Imagery and Mapping Agencies (NIMA) of the USA as well as the German and Italian Space Agencies to generate a near-global DEM of the earth using Radar Interferometry. The SRTM data made it possible to produce the first global DEM of the world (Rabus et al 2003). The African part of the SRTM DEM was released in spring 2004.

The base model consists of one arc-second (30 m resolution) elevation data. The currently available 90 m resolution data are generated by selecting the centre sample of the 3x3 array of one arc-second points surrounding the post location. In other words, for three arc-second data, each point is the average of the nine (9) one arc-second samples surrounding the post location. By doing so, a relatively superior product is produced such that high frequency 'noise' which is characteristic of radar derived elevation data is reduced. This is similar to averaging pixels in radar images to decrease the effects of spackle and increase radiometric accuracy although at the cost of horizontal resolution. Detail regarding the acquisition, processing, interpretation, and limitations of SRTM data are found in Farr (2000) and Rosen et al (2000).

For the Dodoma area, topographic profiles from SRTM-DEM data have been extracted across each fault using the FLEDERMAUS software, at an average spacing of 5 km; the length of each profile was such that it covered both the hanging and the foot walls entirely. The profiles were then used for the computation of scarp vertical offsets and slope differences. The positions of these faults were fine tuned by working interactively within a GIS, where both geology and topographic maps were overlaid in order to decipher faults affecting quaternary deposits from those which do not. Fault parameter computations were then carried out for the entire area. The FLEDER-

suitable for fault parameter computations.

After they were obtained, the vertical offsets were plotted versus the distance along the fault to illustrate the along trend variability of the reference surface relative displacement (displacement profiles).

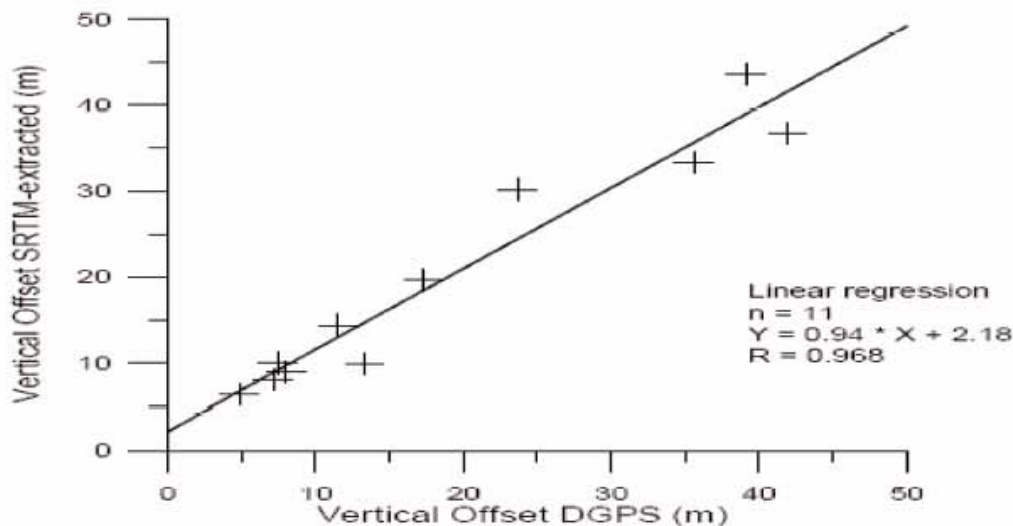


Fig. 4. Comparison between vertical offset obtained from SRTM and DGPS data for profiles which are as close or less than 700 m from each other. Regression line as indicated by correlation coefficient $R=0.968$ shows a good correlation between the two types of profiles.

RESULTS

Structural control

Two main structural trends are clear from the SRTM data and also in the field: 1) NE-trending structures, and 2) NW-trending structures, sub-orthogonal to the former. The resulting architecture is that of a hexagonal shape

The main NE-trending structures are the Saranda, Bubu, Hombolo and Fufu faults, and the main NW-trending structures are the Mponde and Maziwa faults. Most of these faults have relatively impressive fault scarps. Field investigations and SRTM-DEM data interpretation illustrate that the fault scarp heights - and especially those of the NE-trending faults - generally increase towards the north-east.

A cross section from east to west has also shown that there is a general increase in scarp heights from the SE (Hombolo fault) to the NW (Mponde fault). Conversely, there also exists evidence for a gentle regional tilt in the order of 2° towards the east.

Fault parameters

For this particular study, seven faults have been investigated. Of these only four of them have been used to compute the fault parameters. These faults are the Bubu, the Saranda, the Hombolo and the Chikola faults.

Table 1 is a summary of fault parameters for each of

these faults. The table comprises end point UTM36 (ARC1960) co-ordinates for each profile, the corresponding vertical offsets (m), slope difference (°) and the distance (km) of each profile with reference to one end of the fault.

Profile	UTM 36 one end	UTM 36 another end	Slope Difference (°)	Vertical Offset VO (m)	Distance from origin (km)	Fault name
Ddmprof10	0782065E 9413312N	0784318E 9411507N	1.15	103.13	102.48	Bubu
Ddmprof11	0777969E 9409727N	0779742E 9408150N	0.46	121.51	97.73	Bubu
Ddmprof12	0774172E 9406125N	0775962E 9404398N	1.63	126.69	92.75	Bubu
Ddmprof13	0770750E 9402446N	0772562E 9401245N	-1.06	198.61	88.30	Bubu
Ddmprof14	0767092E 9399553N	0768661E 9397574N	0.19	134.67	83.15	Bubu
Ddmprof15	0763362E 9396886N	0764520E 9394827N	1.51	115.72	72.59	Bubu
Ddmprof16	0759248E 9394757N	0760454E 9392493N	-1.28	78.07	68.19	Bubu
Ddmprof17	0754939E 9392544N	0756224E 9389980N	1.01	32.02	63.06	Bubu
Ddmprof18	0751214E 9389658N	0752691E 9386932N	2.00**	43.97	57.68	Bubu
Ddmprof20	0747504E 9386124N	0748809E 9384014N	-0.63	77.44	52.42	Bubu
Ddmprof21	0743240E 9383962N	0744767E 9381978N	-0.58	40.24	47.78	Bubu
Ddmprof22	0739100E 9380735N	0740610E 9378842N	0.42	101.13	42.50	Bubu
Ddmprof23	0735570E 9376777N	0738840E 9372684N	-0.38	50.71	37.90	Bubu
Ddmprof24 W	0731137E 9373559N	0734847E 9370204N	0.80	22.93	33.31	Bubu
Ddmprof24 E	0731137E 9373559N	0734847E 9370204N	0.69	58.04	33.31	Bubu
Ddmprof25	0728111E 9370587N	0731393E 9366119 N	-0.19	47.17	28.30	Bubu
Ddmprof27	0723627E 9360918N	0725768E 9359132N	-1.32	57.28	23.58	Bubu
Ddmprof28	0718727E 9358987N	0722616E 9354783N	-0.24	124.90	18.59	Bubu
Ddmprof29	0716668E 9353991N	0720251E 9350939N	0.37	137.56	13.92	Bubu
Ddmprof30	0714384E 9349055N	0716496E 9347694N	1.67	95.16	8.62	Bubu
Ddmprof31	0711739E 9345275N	0713746E 9343318N	0.62	132.22	3.20	Bubu

Profile	UTM 36 one end	UTM 36 another end	Slope Difference (°)	Vertical Offset VO (m)	Distance from origin (km)	Fault name
Ddmprof33	0701748E 9353381N	0703910E 9351681N	0.45	52.19	0.00	Saranda
Ddmprof34	0704919E 9357753N	0707097E 9355888N	-0.81	55.54	5.23	Saranda
Ddmprof35	0707106E 9362116N	0709743E 9359989N	0.04	28.79	10.30	Saranda
Ddmprof36	0711273E 9366312 N	0713276E 9362852N	0.80	66.48	15.28	Saranda
Ddmprof37	0715187E 9368469N	0716723E 9366903N	0.69	66.48	20.21	Saranda
Ddmprof38	0718671E 9372090N	0720287E 9370357N	-0.26	88.91	25.20	Saranda
Ddmprof39	0721388E 9376358N	0723083E 9374068N	0.63	45.54	29.95	Saranda
Ddmprof40	0724719E 9379736N	0726558E 9377683N	1.16	70.04	34.83	Saranda
Ddmprof41	0727023E 9383953N	0729390E 9382014N	0.43	72.80	39.76	Saranda
Ddmprof42	0728880E 9387336N	0730802E 9386533N	1.48	51.88	44.27	Saranda
Ddmprof44	0734765E 9395460N	0736665E 9393083N	0.49	24.62	53.76	Saranda
Ddmprof48	0825002E 9340968N	0827603E 9338028N	0.01	35.84	8.62	Hombolo
Ddmprof49	0823067E 9336944N	0825112E 9333969N	0.49	28.79	13.14	Hombolo
Ddmprof50	0820677E 9332577N	0822546E 9329994 N	-0.82	16.26	18.14	Hombolo
Ddmprof51	0818107E 9328926N	0820272E 9325687N	0.11	30.62	22.58	Hombolo
Ddmprof52	0815793E 9324626N	0817644E 9320602N	0.19	45.08	28.26	Hombolo
Ddmprof53	0813170E 9320750N	0814491E 9318200N	0.58	27.57	33.10	Hombolo
Ddmprof54	0809647E 9317753N	0810776E 9314115N	-0.07	28.97	37.44	Hombolo
Ddmprofile south2	0769565E 9320195N	0771577E 9321180N	0.08	11.12	2.08	Chikola
Ddmprofile south3	0770739E 9318581N	0771999E 9319279N	-0.30	23.62	4.01	Chikola
Ddmprofile south4	0771947E 9316671N	0773257E 9317972N	-0.24	15.53	6.03	Chikola
Ddmprofile south5	0774043E 9314741N	0774900E 9316000N	0.32	19.40	8.76	Chikola
Ddmprofile south6	0775867E 9313295N	0776793E 9314546N	-0.14	12.36	11.11	Chikola
Ddmprofile south7	0777621E 9311828N	0778066E 9313445N	0.77	21.66	14.92	Chikola
Ddmprofiles outh8	0779282E 9311187N	0779799E 9312759N	0.44	16.61	17.76	Chikola

Table 1. Summary of fault parameters

Displacement profiles and fault segmentation

The Mponde fault

The NW-trending Mponde fault is located west of the Bubu fault and more than 80 km long. This fault hosts a number of hot springs aligned parallel to an antithetic fault for over a distance of 2 km close to its northern extremity. No attempt so far has been undertaken to determine fault segmentation of the fault.

The Bubu fault

The NE-trending Bubu fault has a total length of about 110 km. Geometrically, the fault has three fault segments, i.e. the Nkambala (33 km), Makutupora (30 km) and Gongga (42 km) segments.

The Nkambala fault segment is cross-cut by a nearly 15 km long, ENE-trending fault segment (satellite fault) bifurcating at an angle greater than 20° from the general trend of the Bubu fault (Fig. 5). Beyond the intersection, the Nkambala segment continues further to the NE for about 13 km and dies away.

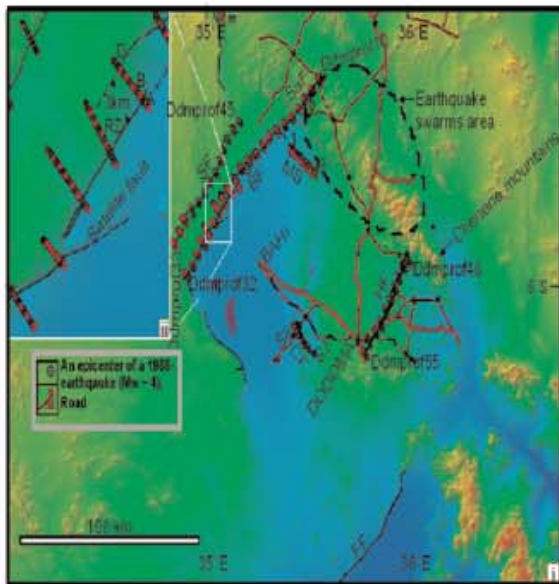


Fig. 5. (i) Location of the SRTM profiles for selected faults. For each fault, only profiles on either ends of any given fault are shown. For instance, for the Saranda fault (SF) which has 13 profiles (Ddmprof33 to Ddmprof45), only Ddmprof33 and Ddmprof45 are shown here. The same applies to the Bubu fault (BF)

and the Hombolo fault (HF). Although the same principle applies to the Maziwa fault (MS) and Chikola fault (CF), the former and the latter are only represented by numerals 1 to 9 and S1 and S8 to represent Ddmprof1 to Ddmprof9 and Ddmprofsouth1 and Ddmprofsouth8 respectively. (See Table 1 for co-ordinates of the profiles and other details). SaF stands for Sanzawa fault line. Earthquake swarms area is characterized by earthquakes with magnitudes >4 but <6 for the period between January 1973 and January 2003. m and g represents Mponde hot spring field and Gongga hot spring field respectively. Faults and inferred faults are respectively represented by solid and dashed lines. RZ stands for relay zone. Note that Bahi is within Bahi depression.

ii) Zoom in the SRTM DEM on a part of the Bubu fault to show the relay zone between the Nkambala fault segment and the Makutupora fault segment. Fault steps A, B and D are also shown (see text for details).

But at this point it has overlapped with another parallel fault segment, the Makutupora segment, which starts 3 km west. Here, the Nkambala and Makutupora segments make up a relay zone. The overlap length is in the order of 8 km, the spacing is 3 km., this configuration could be interpreted as an advanced stage of fault segment linkage (hard linkage?) as shown in figure 6a. There are also some fault steps, mainly in the Makutupora and Nkambala fault segments (see the relationship between steps A and B in relation to C and D, in Fig. 6b).

Further to the NE, the Makutupora segment gives way to the Gongga segment. This is also characterized by at least 4 satellite faults, all of which are sub-parallel to each other. Counting from SW to NE, the first two satellite faults are each ca. 9 km long; the last two each ca. 12-15 km long. The boundary at which the last two satellite faults form is marked by at least half a dozen hot springs, the so-called Gongga hot springs. Their

presence has also been reported in geological maps of Tanzania by the then Geological Survey of Tanganyika e.g. QDS 123 (Kwamtoro, Fozzard, 1961). The hot springs are aligned parallel to the general trend of the fault for about 300 m.

The Saranda fault

The Saranda fault, which is located 10-16 km west of the Bubu fault, runs parallel to the latter for nearly 40 km before it changes to a its direction and assumes a NW-trendoriented strike. After this point it is called the 'Mponde fault'. The Saranda fault is nearly 55 km long and can be subdivided into three main fault segments

based on the displacement profile plots: i.e. the Saranda South (at least 11 km), Saranda Mid (29 km) and Saranda North (24 km) fault segments. Like the Bubu fault, this fault also displays some fault steps along its length. However, unlike the former, the fault steps are not restricted to any fault segment but generally continue along the entire length of the fault (Fig. 7).

An important observation is that the position of the displacement profile minima between the Saranda Mid and Saranda North segments occurs at approximately the same position (transversely) as those between the

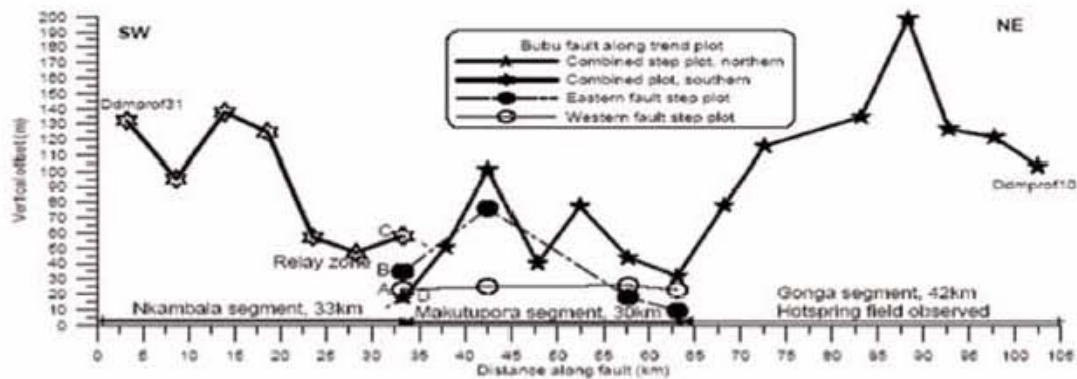


Fig. 6a. Displacement profile for the Bubu fault. The fault is slightly longer than 105 km. Dashed lines infer the possible VO for that part of the observed fault. Profiles involved in calculations of VO are from Ddmprof10 to Ddmprof 31 (See Fig. 6 and Table 1 for locations of profiles). The sum of A and B equals C, see Fig. 6b for details.

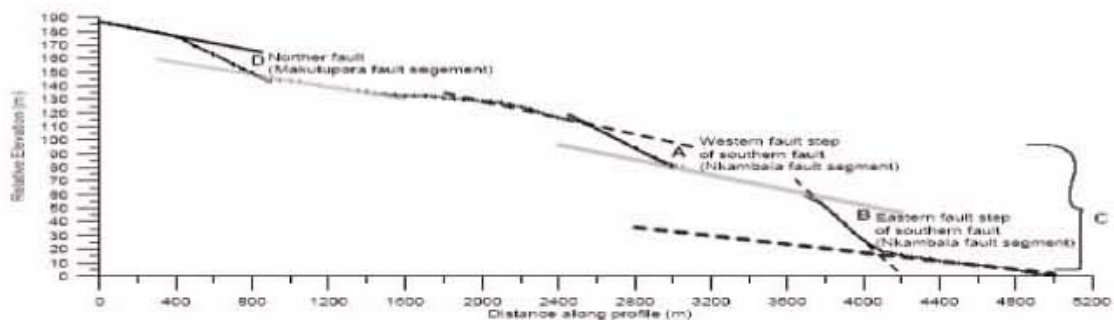


Fig. 6b. Relative elevation versus distance across both the Nkambala and the Makutupora fault segments (Ddmprof24, see also Fig. 6 and Table 1). Three fault steps, D, A and B (naming from west), can be clearly seen. Note that the lines drawn parallel to each other, whether solid or dashed, at D, A and B are reference lines which represent upper and lower reference surfaces. The fault steps vertical offsets A and B equals C (See Fig. 6a for location).

Nkambala and Makutupora segments of the parallel Bubu fault (Fig. 6). This could indicate the presence of a significant NW-oriented structural discontinuity across both faults.

The Hombolo fault

The Hombolo fault is about 40 km long. It is a NW-dipping fault, i.e. antithetic to all other normal faults in this area. It is less impressive, characterized by only a gentle slope. It runs through the Hombolo area and hosts the famous Hombolo dam. The fault has systematically been affected by erosion in two major directions, NW and SE. This erosion seems to be accelerated by both the NW slope of the fault scarp and the slope due to easterly tilt of the entire area. This tilt is considered to be regional since a SRTM profile drawn from

west of the Saranda fault to east of the Hombolo fault clearly reveals a tilt in the order of 2°. The Hombolo fault has two fault segments: i.e. the Dam (≥ 18 km) and the Nzuguni (> 19 km) fault segments (Fig. 8). The Dam fault segment locally shows 2-3 fault steps, which might be attributed to a paleo-landslide(s).

The Fufu fault

Like many of the faults in the Dodoma area, the Fufu fault is an impressive fault, with scarp heights ranging from less than 20 m in the last 8-10 km to the north (where its general trend is nearly N-S) to over 50 m in the south (main scarp). Fault steps are not uncommon on the main scarp. Like in the Mponde fault, no attempt so far has been made so far to determine fault segmentation of the fault.

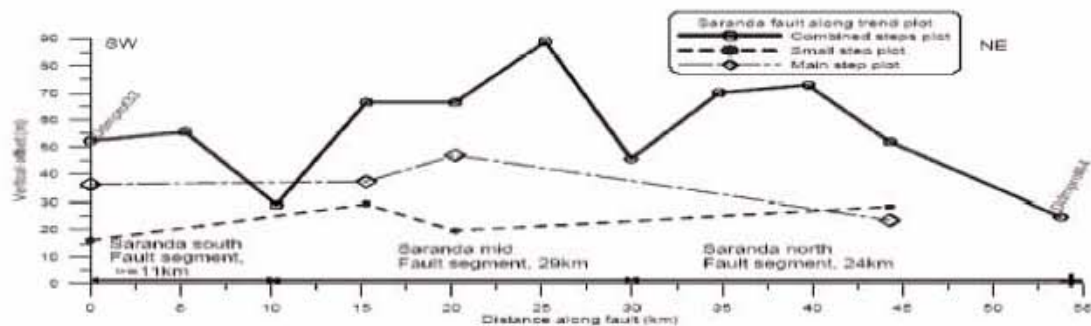


Fig. 7. Displacement profile for the Saranda fault. Note that this plot is for the profiles Ddmprof33-44. However, profile Ddmprof43, is not used in the plot (See also Fig. 6 and Table1).

The Chikola fault

The Chikola fault is located in the south-western part of the study area within and parallel to the southeastern end of the Bahi depression (Fig. 9). The SRTM data and field check show that the scarp of this fault is much lower than that of other faults in this area. Results also show that unlike all other faults in this area, its vertical offset (displacement) decreases towards its centre, contrary to the typical displacement profile (e.g. Burbank and Anderson, 2001). A possible explanation for this unusual displacement profile is provided further on, in the discussion section.

The Maziwa fault

The Maziwa fault is another NW-trending linear structure that occurs mainly between the Bubu and the Hombolo fault. It is weakly expressed on the surface and shows no particular slip pattern. Results from SRTM DEM data show that the structure cuts through recent sediments within the Bahi depression and that it joins or intersects the Gongga fault segment at Magungu, within the Bubu fault (Figs 6).

Some SRTM profiles across the structure indicate a dip-slip sense (Fig 10). On the other hand, rivers or

streams tend to be deflected dextrally on one side of it. However, field checks at two points located about 3 km away along the structure at or around the Maziwa village revealed no data to support the observations highlighted above. This is probably because no outcrops are visible around both points due to a thick siliceous cover (known as the Kilimatinde cement, a silicate weathering product composed of kaolinite and silica) on and across which the Maziwa structure passes. Due to the aforesaid reasons, neither vertical offsets were calculated nor were displacement profiles established across this fault.

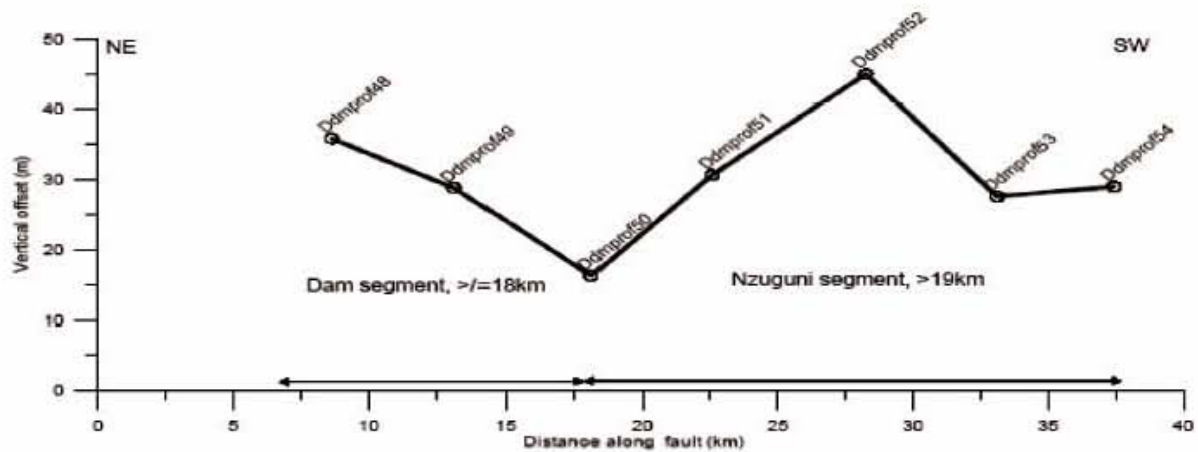


Fig. 8. Displacement profile for the Nzuguni. All profiles used for the computation of vertical offsets are used. (See also Table 1 and Fig. 6 for locations).

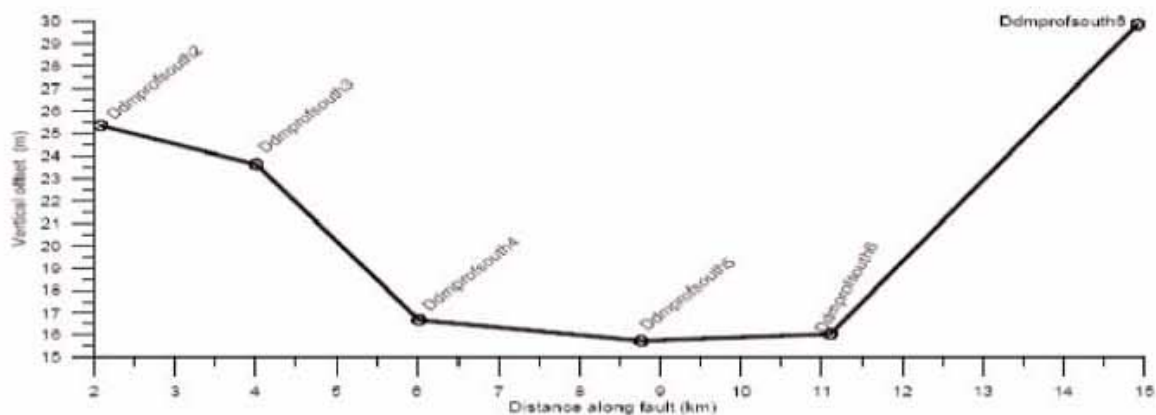


Fig. 9. Displacement profile for the Chikola fault. All profiles used for the computation of vertical offsets are used. (See also Table 1 and Fig 6 for locations).

Hot springs

Hot springs have been found both in the Gonga and Mponde areas. The hot springs at Mponde are along a small antithetic parallel fault to the main Mponde fault, whereas those at Gonga are parallel and within the Gonga fault segment, which is part of the Bubu fault. The hot springs at Mponde physically cover a strike length of at least 2 km, whereas those at Gonga can be mapped along strike for up to 400 m.

Whether coincidental or not, these hot springs are confined to the western margin of the Chenene mountains, which is thought to be cut by the NW-SE Sanzawa fault. The latter is parallel with the Maziwa fault.

geometric criteria on determination of fault segments have a low to moderate likelihood of being or corresponding to earthquake segments (McCalpin 1996). Thus, in order to enhance fault segment determination, the delineation of minima and maxima using along-strike displacements of each fault has to be integrated to a large extent with the geometry of individual faults.

The results presented here reveal generally three major fault segments along the Saranda and the Bubu faults, two fault segments along the Hombolo fault and at least one fault segment associated with the Chikola fault. Based on the total lengths and the mean vertical offsets (Table 1) of each fault it can be concluded that no single earthquake event could have generated any one of

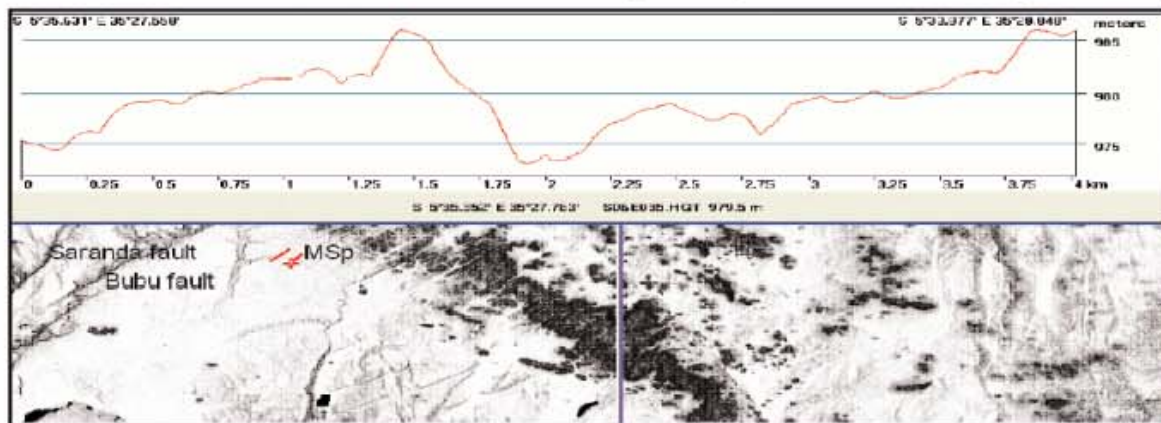


Fig. 10. A profile across the middle part of the Maziwa fault as extracted from SRTM DEM. The end points of the profile are defined by the latitude and longitudes, $S5^{\circ}35.631'/E35^{\circ}27.558'$ and $S5^{\circ}33.877'/E35.28.848'$. MSp stands for the Maziwa fault profile.

DISCUSSION

Vertical offset minima along faults, as revealed by our topographic profiles (e.g. Fig. 7-10), can be interpreted to represent points at which fault segments have linked during fault growth (Peacock and Sanderson 1991; Young et al 2001). However, according to Burbank and Anderson (2001), the choice of fault linkage positions using simple along-strike displacement variations is relatively difficult and needs to be substantiated with summed slip deficit. Furthermore, at the absence of observed or deduced surface rupture evidences,

these faults (Wells & Coppersmith 1994), i.e., multiple earthquake events must have been responsible for the formation of these faults and their present relief.

The genesis of these faults is detailed elsewhere but just to highlight; it is most likely that several individual fault segments nucleated in isolation (discretely) and became connected later on in their evolution as they continued to grow laterally (Burbank and Anderson 2001). At some stages, in the process of growth, they overlapped, started to interact, got hooked and finally

became linked together to their tips (Young et al 2001). The resulting displacements (vertical offsets) are now seemingly much higher than that of the individual fault segments. As earthquakes continue to strike the area, there is no doubt that this process of fault growth is still in action. Similar conclusions were drawn by Shudofsky (1985). However, the vertical offset versus fault length ratio is generally much more reduced than before fault interactions (Wash et al 2002).

Interestingly, the vertical offset (displacement) along the Chikola fault decreases towards its centre, contradicting the Burbank and Anderson (2001) theory, which requires that ordinarily the fault or fault segment would have maximum displacement at its center. Such an anomalous profile, however, may have simply resulted from fault interactions that distorted fault slip profiles, resulting in a fault with such distinctive characteristics (Peacock and Sanderson 1991).

On the other hand, such a fault could have resulted from internal deformation of blocks that are found on either side of the fault (e.g. Jackson and White 1989). As this area is structurally complex, with faults of different orientations and some faults cross-cutting each other, fault interactions (such as internal deformations) are possible. As the Chikola fault is sub-orthogonal to and intersected by several NE-trending structures, part of the stress responsible for its growth is most likely taken up by these structures, hereby negatively affecting its vertical offset or displacement. This complexity can be reflected in the displacement profile of the fault.

Further to this, the role played by pre-existing Precambrian structures, along which these Quaternary faults have developed by reactivation, cannot be ignored. According to the Burbank and Anderson (2001) theory, reactivated faults may pose ambiguity in inferring the stress field orientation in relation to the

orientation of active faults. Stress field orientation is an important element to be borne in mind for analysis of fault displacement and morphology (Angelier 1989).

Hot springs can be good indicators of active tectonics, in particular when they appear to assume a particular trend, usually a linear one. They reveal the lines or zones of weakness through which water from deeper parts of the crust reach the surface. The presence of these structurally controlled hot springs seems to confirm that this area, particularly the Bubu and the Mponde (Saranda) faults, is indeed seismically active.

The fact that this area on the Tanzanian craton is seismically active somewhat attracts the attention to review the definition of 'craton', which in principle is supposed to be tectonically stable since Archaean. One of the possible explanations however could be that these active faults, though found on the craton, are essentially restricted to the fractured craton margins thus chances for fracturing it further through the pre-existing fractures are high because the frictional strength necessary to form a fault on a pre-existing structure is less than the stress necessary to form a new one (Angelier, 1989; Wash et al 2002).

Fault segments located in the north of the area and which are long enough, such as the Bubu fault, effectively show vertical offsets increasing towards the north. Deformation away from the craton center is relatively higher and indeed so severe outside the craton. The Pangani rift for that matter, is an example.

In this study, a new structure has been reported for the first time: the Maziwa fault, ca. 30 km long. Although we do not provide much information about its sense of displacement (and/or fault kinematics), segmentation, vertical offsets, etc., there are indications that this structure laterally (most likely dextrally) displaces Quaternary deposits and hence opens a subject for

further paleoseismic investigation (s). It would be worth to preliminarily highlight that such a fault could be a release fault or a cross-fault that accommodates differences in strain or structural styles along the strike of the extensional system (Gibbs, 1984; Destro, et al 2003), and in our case, between the Bubu and Hombolo faults.

Another structure is observed to be parallel to the Maziwa structure as is shown by the SRTM data DEM. It runs across the NE-trending Bubu and Saranda faults. Such NW-trending structures, if considered active, may have a significant contribution towards buffering of the system by accommodating part of the deformation. Thus the possible earthquake magnitudes reported so far in this paper may not necessarily be attained. Such sub-orthogonal structures may on the other hand act as geometric discontinuities and/or structural discontinuities within a fault zone (Zhang et al 1998). They can potentially influence earthquake rupture initiation and termination, and may impede or stop earthquake rupture propagation (Zhang et al 1998).

We wish to point out, however, that it is not possible to distinguish whether a geometric discontinuity is a real seismic barrier or not based solely on its geometry, as the behavior of the fault step will be completely different in case the faults are connected at depth to a single one, or in case for example, the zone between the two faults consists of already heavily fractured, or easy to fracture materials (Harris and Day 1993).

For more precise and detailed studies of displacement profiles, the 90-m-resolution SRTM data profiles need be supplemented by more precise data such as those from differential GPS, Total Station and electric tomography. The results obtained from 90 m SRTM data give only basic clues for relatively but not limited to regional interpretations.

CONCLUSION AND RECOMMENDATION

Communities living in the Dodoma area need to be aware of the fact that large, damaging ($M_w = 6.3-6.9$) and major, destructive ($M_w = 7.0-7.2$) earthquakes are likely to be generated by the investigated faults, leave alone the fact that moderate earthquakes ($M_w < 6.0$) are common in the area. The recurrence rate of these earthquakes, however, requires more detailed paleoseismic investigations.

According to the empirical relations between earthquake magnitudes, rupture length, rupture width, rupture area and surface displacement, (Wells & Coppersmith 1994), the possible maximum earthquake magnitudes which can be generated by these fault segments, assuming full re-activation of each individual fault segment, is summarized in Table 2. However, when all fault segments from an individual fault are re-activated, then much larger earthquakes are possible. For the Bubu (110 km), Saranda (55 km) and Hombolo (40 km) faults, the maximum possible earthquake magnitudes are of the order of $M_w = 7.2$, 7.1 and 6.9, respectively. Actually, the possible earthquake magnitude for the Bubu fault would be $M_w = 7.4$, but the fact that there is a significant geometric discontinuity reduces the chances for all the three segments to be ruptured at once. In other words, we believe that the relay zone of about 3 km wide between the Nkambala and the Makutupora segments is a structural discontinuity which might be enough to potentially act as a structural barrier that could impede or stop earthquake rupture propagation. Thus effectively, the longest possible fault is in the order of 70 km, which is the total length of both the Makutupora and Gongga fault segments. In addition, the presence of the minimum in displacement value between the Saranda Mid and the Saranda North fault segments at approximately the same position (transversely) as that between the Nkambala and Makutupora fault segments, suggests the presence of a significant structural discontinuity across both faults

and this may also impede or stop earthquake rupture propagation more northerly.

Finally, in order to come out with up dated geo-hazard maps on the area, research work focused at characterization of active faults and constrain the age relationship of the same for various geologic events in this particular area is/are strongly recommended.

Acknowledgement: This work is being supported by Belgium Technical Cooperation and the Government of the Republic of Tanzania. Many thanks are due to L. Naudts of Renard Center for Marine Geology,

Universiteit Gent, for technical assistance in the use of the Fledermaus program. We are indebted to S. Abel and D. Nhigula from the Mineral Resources Institute in Dodoma for their technical assistance in the field and to E. B. Temu and F. Nyanda Petro, both from the Geological Survey of Tanzania, for the assistance in the regional geological framework of the study area. Furthermore, Mr. Temu is thanked for his remarkable field logistics and recommendations on the Dodoma area. We are indebted to D. Gabriel for providing us with access to some useful references. Damien Delvaux is supported by the Belgian Federal SPP Science Policy.

Fault / Fault segment	Fault Length (km)	Maximum fault Displacement (m)	Maximum magnitude of potential earthquake (M_w)
Hombolo / Dam	18	0.55 - 0.76	6.5 - 6.6
Hombolo / Nzuguni	> 19	0.55 - 0.76	6.5 - 6.6
Bubu /Gonga	42	~ 2.62	~ 7.0
Bubu / Makutupora	30	~ 1.41	~ 6.8
Bubu / Nkambala	33	1.41	6.8
Saranda / Saranda South	11	0.30	6.3
Saranda / Saranda Mid	29	1.41	6.8
Saranda / Saranda North	24	1.03	6.7

Table 2. Maximum possible earthquake magnitudes (M) which can be generated by these fault segments, assuming fully reactivation of each individual fault segment in accordance with Wells & Coppersmith (1994). L and D respectively stand for fault length and vertical offset (synonymous to fault displacement).

REFERENCES

1. **Angelier, J.**, 1989. From Orientation to Magnitudes in Paleostress Determinations Using Fault Slip Data. *J. Struc. Geol.* 11(1-2), 115-137.
2. **Baker, B.H.**, 1965. An outline of the Geology of the Kenya rift valley. Rep. UMC/UNESCO Seminar on the East African Rift System (Nairobi).
3. **Bell, K., Dodson, H.S.**, 1981. The Geochronology of the Tanzania Shield – *J. Geol.* 89(1), 109-128, Chicago.
4. **Barth, H.**, 1996. Gold in the Dodoman basement of Tanzania, pp.1-53, Hanover.
5. **Brazier, R.A., Nyblade, A.A. and Florentin, J.** (2005). Focal mechanisms and stress regime in NE and SW Tanzania, East Africa. *Geophysical Research Letters*, 2005, 32/14 (1-4).
6. **Brown, C., Girdler, R.W.**, 1980. Interpretation of African Gravity and its implication for the breakup of the continents. *J. Geophys. Res.* 85, Ba, 6443-6455.

7. Burbank, D.W., Anderson, R.S., 2001. Tectonic Geomorphology. Blackwell Science: USA. Pp: 33, 43, 105-129.
8. Cartwright, J.A., Trudgill, B. D., Mansfield, C.S., 1995. Fault growth by segment linkage: an explanation for the scatter in maximum displacement and trace length data from the canyonlands grabens of SE Utah. *J. Struct. Geol.* 17, 1319-1326.
9. Crone, A.J., Haller, K.M., 1991. Segmentation of Basin and Range normal faults: examples from east-central Idaho and southwestern Montana. *J. Struct. Geol.* 13, 151-164.
10. Destro, N., Alkmim, F.F., Magnavita, L.C., Szatmari, P., 2003. The Jeremoabo transpressional transfer fault, Reconcavo–Tucano Rift, NE Brazil. *J. Struct. Geol.* 25, 1263–1279.
11. Rabus, B., Eineder, M., Roth, A. Bamler, R., 2003. The shuttle radar topography mission—a new class of digital elevation models acquired by spaceborne radar ISPRS. *J. Photogrammetry and Remote Sensing*, 57(4), 241-262.
12. Fairhead, J.D., Stuart, G.W., 1982. The seismicity of the East-African rift system and comparison with other continental rifts. In: Palmason, G. (ed.): Continental and Oceanic Rifts. - Geodynamic Series, 8: 41-61.
13. Farr, T.G., Kobrick, M., 2000. Shuttle Radar Topography Mission produces a wealth of data. *Amer. Geophys. Union Eos.* 81, 583-585.
14. Fozzard, P.M.H., 1960. Geological Survey of Tanzania. 1:125.000 Geological map Quarter Degree Sheet 124 Kelema. Geological Survey Division, Dodoma.
15. Fozzard, P.M.H., 1961. Geological Survey of Tanzania 1:125.000 Geological map Quarter Degree Sheet 123 Kwa Mtoro. Geological Survey Division, Dodoma.
16. Fozzard, P.M.H., 1962. Brief explanation of the Geology of QDS177 Manzoka-Geological Survey of Tanganyika, pp. 1-7, Unpublished Report, Dodoma.
17. Gabert, G., 1973. Über Granitische Gesteine des Dodoman und Usagaran im Sudlichen Hochland von Tanzania. *Geological j.* b6: 1-50 Hanover.
18. Gabert G., Wendt, I., 1974. Datierung von Granitischen Gesteinen im Dodoman -und Usagaran System und in Der ndembera-serie (Tanzania). *Geological j.* b11: 3-55, Hanover.
19. Gibbs, A.D., 1984. Structural evolution of extensional basin margins. *J. Geol. Society* 141, 609-620.
20. Harris, R.A., Day, S.M., 1993. Dynamics of fault interaction: parallel strike-slip faults. *J. Geophys. Res.* 98, 4461– 4472.
21. Iranga, M.D., 1991. An earthquake catalogue for Tanzania, 1846-1988. University of Dar Es Salaam, Seismological department report No. 1-91, 80pp.
22. Jackson, J.A., White, N.J., 1989. Normal faulting in the upper continental crust: observations from regions of active extension. *J. Struct. Geol.* 11 (1-2), 15-36.
23. Julian, W., Lounsberry, W., Tamura, A., Van Loenen, R., Wright, M.P., 1963. Geological Survey of Tanzania. 1:125,000 Geological map Quarter Degree Sheet 143 Meia Meia. Geol. Survey Division, Dodoma.
24. Keller, A. and Pinter, N., 2002. Active tectonics. Earthquakes, Uplift and Landscape. 2d ed. Prentice Hall Earth Sciences Series, New Jersey. 362pp.
25. Lounsberry, W., Van Loenen, R., Wright, M.P., U.S.A. Peace Corps 1963 and Haslam, H. W., 1967. Mineral Resources Division, Tanzania. 1:125.000 Geological map Quarter Degree Sheet 142 Bahi. Geological Survey Division,

- Dodoma.
26. **McCalpin, J.P. (Ed.)**, 1996. Paleoseismology. Academic Press, New York. 583 pp.
 27. **Peacock, D. C.P., Sanderson, D.J.**, 1991. Displacements, sediment linkage and relay ramps in normal fault zones. *J. Struct. Geol.* 13, 721-733.
 28. **Piccardi, L.**, 2005. Paleoseismic evidence of legendary earthquakes: The apparition of Archangel Michael at Monte Sant' Angelo (Italy). *Tectonophysics* 408, 113–128.
 29. **Pinna, P., Muhongo, S., Mcharo, A., Le Goff, E., Deschamps, Y., Ralay, F., Milesi, J.P.**, 2004. A 1: 2, 000, 000 Geology and mineral map of Tanzania. Presented in the framework of the 20th colloquium of African geology (2-7 June, 2004 BRGM Orléans, France).
 30. **Rosen, P.A., Hensley, S., Joughin, I.R., Li, F.K., Madsen, S.N., Rodriguez, E., Goldstein, R.M.**, 2000. Synthetic Aperture Radar Interferometry, *Proc. IEEE*, 88: 333-382.
 31. **Shudofsky, G.N.**, 1985. Source mechanisms and focal depths of East African earthquakes using Raleigh-wave and body wave modeling. *Geophysical J. Royal Astronomical Society* 83: 563–614.
 32. **Thomas, M.F.**, 1994. Geomorphology in the tropics. A study of Weathering and Denudation in Low Latitudes. Wiley, Chichester. Singapore. 460 pp.
 33. **Vocht, M., Kröner, A., Poller, U., Sommer, H., Muhongo, S. and Wingate, M. T. D.**, 2006. Archaean and Palaeoproterozoic gneisses reworked during a Neoproterozoic (Pan-African high-grade event) in the Mozambique belt of East Africa: Structural relationships and zircon ages from Kidatu area, central Tanzania. *J. Afr. Earth Sci.* 45(2), 139-155.
 34. **Wades, F.B., Oates, F.**, 1938. An explanation of degree sheet no. 52, Dodoma-Geological Survey of Tanganyika. Short paper 17, 1-60, Dar es Salaam.
 35. **Wash, J.J., Nicol, A. Childs, C.**, 2002. A new model for the growth of faults. EAGE 64th Conference & Exhibition-Florence, Italy.
 36. **Wells, D.L., Coppersmith, K.J.**, 1994. New empirical relations among magnitude, rupture length, rupture width, rupture area and surface displacement. *Bull. Geol. Seism. Soc. Am.* 84, 974-1002.
 37. **Wendt, I., Besang, C., Kreuzer, H., and Muller, P.**, 1972. Agedetermination of Granitic Intrusions and Metamorphic Events in the Early Precambrian of Tanzania-24th International Geological Congress, Section 1; 295-314: Montreal.
 39. **Young, M.J., Gawthorpe, R. L., Hardy, S.**, 2001. Growth and Linkage of a segment normal fault zone; the Late Jurassic Murchison-Statfjord North Fault, northern North Sea. *J. Struct. Geol.*, 23, 1993-1952.
 40. **Zhang, P., Mao, F., Slemmons, D.B.**, 1998. Rupture terminations and size of segment boundaries from historical earthquake ruptures in the Basin and Range Province. *Tectonophysics*. 308, 37-52.